Biointerface Research in Applied Chemistry
Platinum Open Access Journal (ISSN: 2069-5837)

Article
Volume 10, Issue 5, 2020, 6460 - 6473
https://doi.org/10.33263/BRIAC105.64606473

Electrochemical Detection of Dopamine and Tyrosine using Metal oxide (MO, M=Cu and Ni) Modified Graphite Electrode: a Comparative Study

Budde Kumara Swamy [1], Kudekallu Shiprath [1], K. Venkata Ratnam[1], H. Manjunatha [1*], Sannapaneni Janardan [1], A. Ratnamala [1], K. Chandra Babu Naidu [2], S. Ramesh [2], Kothamasu Suresh Babu [3]

[1] Department of Chemistry, GITAM School of Sciences, GITAM (Deemed to be University), Bengaluru, Karantaka, India
[2] Department of Physics, GITAM School of Sciences, GITAM (Deemed to be University), Bengaluru, Karantaka, India
[3] Department of Humanities & Sciences, Marri Laxman Reddy Institute of Technology and Management, Hyderabad,Telangana, India
* Correspondence : hanumanjunath80@gmail.com;

Scopus Author ID 57188956297
Received: 25.04.2020; Revised: 10.05.2020; Accepted: 11.05.2020; Published: 13.05.2020

Abstract: An electrochemical oxidation of dopamine (DA) and tyrosine (Tyr) by metal oxide (MO) modified electrode where M=Cu and Ni in phosphate buffer solution (PBS), pH 7.0 has been studied by cyclic voltammetry (CV) and differential pulse voltammetry (DPV) techniques. CuO and NiO nanoparticles were prepared by sol-gel process and co-precipitation method respectively and their structure, composition and surface morphology were examined by SEM, XRD, FTIR, UV and Raman techniques. A simple drop cast method is employed for the surface modification of graphite electrode to prepare MO modified electrode and it exhibited good electrocatalytic activity towards detection of DA and Tyr. The present investigation on CV studies of DA at CuO modified electrode showed a reversible oxidation process with an anodic peak potential at +0.249V vs. SCE. However, no specific anodic oxidation peak identified with NiO modified electrode. Subsequent CV studies with Tyr at MO modified electrode (M=Cu, Ni) shows an irreversible oxidation process and both modified electrodes exhibited an anodic peak at a potential of +0.80V against very low or no anodic peak currents obtained at bare graphite electrode. Moreover, the CuO modified electrode (CMG) successfully separated the anodic signals of dopamine (DA), Ascorbic acid (AA) and Tyrosine in their ternary mixture whereas on bare graphite a single, overlapped oxidative peak was observed. In CV studies, the peak potential difference between AA-DA, DA-Tyr and AA-Tyr is 166 mV, 323 mV and 489 mV respectively and the corresponding peak potential separations are 209 mV, 400 mV and 609 mV respectively in differential pulse voltammetry (DPV). Owing to good stability, selectivity and simple low cost fabrication method, CuO modified electrode is found to be well suited for simultaneous determination of DA, AA and Tyr in their ternary mixture. Additionally, NiO modified electrode also shows good sensitivity towards the detection of tyrosine, so it acts as a good electrochemical sensor to assay tyrosine in the biological sample.

Keywords: MO modified graphite electrode; Dopamine; Tyrosine; Ascorbic Acid; Drop cast method;Cyclic voltammetry; Differential Pulse voltammetry.

1. Introduction

A noteworthy technological change has been noticed over the years in the sensing of neurotransmitters owing to their predominant role as a diagnostic tool in medicine to forecast specific metabolic diseases [1-2]. In mammalian brain tissues, the occurrence of

neurotransmitters not only meant for a specific metabolic activity but also as biological indicators to identify the state of a disorder or disease [3-4]. It is very clear that a disharmony in the release of neurotransmitters like dopamine and tyrosine always engender for metabolic and neurological disorders [5]. In the family of catecholamine-neuro transmitters, dopamine (DA) has occupied pinnacle position in stating physiological functions belonging to hormonal, renal, neural and cardiovascular systems in the human body. So its role is pivotal and its abnormal levels in the blood are a cause of concern for diseases like Huntington's disease, Schizophrenia and Parkinson's disease etc [6-8]. In addition, tyrosine (Tyr), a precursor of dopamine plays an essential role in causing inborn disorders like Alkpatonuria (AKU), Tyrosinaemia (I, II and III type) and Hawkinsinuria. To envisage type-2 diabetes, liver cancer and obesity the concentration level of tyrosine play a decisive role [9-10].

On contemplating the method of estimation of dopamine and tyrosine, electrochemical methods were phenomenal in spite of a plethora of other analytical techniques available. Portability, accuracy and fast response in sensing, electrochemical methods are better than any other analytical methods which have their own setbacks [11-13].At present, the augment of new materials still continue to be of interest to apply on the surface of graphite electrode with better sensing properties, including conductive polymers, nanoparticles and carbon based materials. More recently, the sensors based on various metal oxide nanoparticles have evinced to be more efficient due to high selectivity, sensitivity, low cost, easy to synthesize in various nanostructures and excellent electro-active nature [14-17]. Such chemically modified electrodes are well suitable in resolving the homogenous structures like dopamine and tyrosine at different electrode potentials though both coexist at low concentrations [18]. So the challenges prevailed even in electrochemical methods like maintaining stability sensitivity and selectivity in the detection of target molecules like dopamine and tyrosine in the presence of other interference molecules [19-23].

In the search of metal oxide nanoparticles, copper (II) oxide (CuO), a p-type of semiconductor with a band gap of 1.2 to 2.2 e V has been showing countless applications including electrochemical sensors, gas sensors, life aspects, solar energy, batteries and green catalysts [24-27]. The copper oxide nanoparticles can be prepared in various morphological shapes such as nanowires, platelets and spindles [28-29]. In the detection of glucose [30-31] and other biomolecules [32-37], copper oxide nanoparticles were of extremely useful. On the other hand, nickel (II) oxide (NiO) nanoparticles exhibits a band gap of around 3.7eV and is a p-type semiconductor. Because of low toxicity, good stability and high electrocatalytic property, NiO nanoparticles attracted the attention of many researchers in the field of electrochemical sensing and lured electrochemists a lot [38-41]. Despite its own limitations, NiO nanoparticles have been used to sense certain electro-active bio-molecules like dopamine and others, which support the research reports [38-40].

In this study, CuO and NiO nanoparticles were prepared by sol-gel process and co-precipitation method respectively and characterized by XRD, UV, IR, Raman and SEM techniques. From the available literature and to the best of the authors knowledge, electrochemical studies on dopamine and tyrosine using CuO and NiO nanoparticles are scanty and a comparative study on the electrochemical performance of CuO and NiO nanoparticles modified graphite electrode towards oxidation of dopamine and tyrosine is not reported.

2. Materials and Methods

2.1. Reagent and materials.

Dopamine, ascorbic acid, copper (II) nitrate, nickel (II) chloride, NaOH, ethanol and liquid paraffin were purchased from Sigma-Aldrich. Potassium chloride, potassium dihydrogen phosphate, dipotassium hydrogen phosphate, tyrosine were purchased from Fischer Scientific Ltd. and used as received. Stock solutions of 0.01M dopamine, 0.01M ascorbic acid and 0.002M tyrosine were prepared freshly using double distilled water. Phosphate buffer solutions (PBS) were prepared from stock solutions of 0.1M K_2HPO_4, 0.1M KH_2PO_4. All other chemicals were of analytical grade and used without further purification.

2.2. Equipment.

The prepared CuO and NiO nanoparticles were physically characterised by Powder X-Ray Diffraction (XRD) using X'Pert PRO Diffractometer with Cu Kα radiation of wave length 0.15406 nm. The surface morphology of the synthesised particles of NiO and CuO were observed using a scanning electron microscope (SEM) HITACHI S4160. Fourier transforms infrared (FT-IR) spectra and UV-Vis spectra of the material were recorded using Thermo model, Instrument model λ 35, to determine the functional groups. Raman spectra of the material at room temperature (RT) were obtained using 3D scanning confocal microscope with spectrometer nanofinder-S (SOLAR TII, Ltd.).

2.3. Electrochemical measurements.

The electrochemical measurements such as cyclic voltammetry (CV) and differential pulse voltammetry (DPV) were carried out using a potentiostat/galvanostat, VSP, Biologic's instruments, France. A three electrode electrochemical cell consisting of MO (M=Cu or Ni) modified graphite electrode as a working electrode , a platinum wire as auxiliary and a saturated calomel electrode as reference electrode was used for all electrochemical measurements with 0.1 M phosphate buffer solutions (PBS) with 0.1M KCl as supporting electrolyte.

2.4. Synthesis of MO (M=Ni and Cu) nanoparticles (NPs).

2.4.1. Copper oxide NPs.

CuO nanoparticles were prepared by sol-gel method which involves reacting two aqueous solutions of 100ml 0.1M of Cu $(NO_3)_2$ .3 $H_2O$and NaOH 0.9 Msolution (pH=13 at 25° C). 0.9 M NaOH solution was added to 0.1 M of Cu $(NO_3)_2$.3 H_2O solution drop by drop until a blue gel was produced. The obtained gel was washed several times with distilled water until it is free from nitrate ions. It was then centrifuged and dried in air at 60 °C for 12 hrs. This dried gel was separated in several portions and annealed in air for 3 hrs at 250 °C.

$$Cu(NO)_2 + 2NaOH \longrightarrow Cu(OH)_2 + 2NaNO_3$$
$$Cu(OH)_2 \longrightarrow CuO + H_2O$$

2.4.2.Nickel oxide NPS.

Nickel oxide nanoparticles were prepared by co-precipitation method. In atypical procedure, 2.6 g of nickel(II)chloride was dissolved in 100 ml of de-ionized water. To this, sodium hydroxide (4 g in 100 ml of deionized water) solution was added drop by drop under constant stirring up to 4 hrs.The resultant solution was kept under refluxed at room temperature for 24 hrs. The obtained green precipitate was washed with double distilled water and ethanol 5-6 times to remove any possible ionic remnants if formed. The sample was dried by heating at 90°C. The same is then calcinated at 250°C when the greenish sample turned into black color powder.

$$NiCl_2.6H_2O + H_2O + 2NaOH \longrightarrow NiO + 8H_2O + 2NaCl$$

2.5. Preparation of MO (M=Ni or Cu) modified graphite electrode.

A Teflon bar with 6mm internal diameter was fitted with a spectroscopic grade pure graphite (6mm diameter) purchased from Sigma-Aldrich. The surface of graphite electrode was activated before modification by polishing with emery papers of different grades like 1000 and 800 to get a mirror shining surface. Further, it was cleaned by sonication with double distilled water for 2 minutes. A MO suspension was prepared by mixing 5 mg of MO nanoparticles in 0.1 ml of liquid paraffin and 0.9 ml of water by sonicating the mixture for 30 minutes. The obtained homogenous black suspension of about 10µL was dropped on cleaned surface of graphite electrode and allowed to dry for about 3 hrs at room temperature [41]. The resulting modified electrode acts as a working electrode and from here onwards referred to as MO/Gr (M=Ni or Cu) modified electrode.

3. Results and Discussion

3.1. Characterization of MO (M=Cu and Ni) nanoparticles.

3.1.1. XRD Studies.

The XRD pattern of the prepared CuO and NiO nanoparticles are shown in Fig.1 (A) and Fig.1 (B). In Fig.1 (A) the appeared diffraction peaks at 2θ= 32.83, 35.53, 38.68, 48.93, 53.46, 58.18, 61.72, 66.26, 68.23, 72.56 and 75.12 correspond to the lattice planes, (110), (11-1, 111), (20-2), (202), (11-3), (022, 31-1), (220),(311) and (004,22-2) respectively . All peaks can be well indexed to monoclinic symmetry with a space group of C^6_{2h} and are in consistent with standard (JCPDS file no. 45-0937) data. In Fig. 1(B), XRD of NiO nanoparticles has three distinct peaks at 2θ = 36.5^0, 43.5^0 and 63^0 with peak line broadening indicating nano particle size of NiO material. The prominent peaks are indexed as (111), (200), (220), (311) and (222) which correlate to face-centered cubic (*FCC*) structure of NiO phase and are in good agreement with standard (JCPDS -file: 78-0429, *Fm3m* space group) data. The particle size of metal oxide (MO, M=Cu and Ni) nanoparticles were calculated using Debye-Scherer's formula shown below with k-0.9, Scherrer's constant, λ- wavelength of the Cu-Kα radiation (1.5406 Å),

$$d = K\lambda / (\beta \cos \theta) \qquad (1)$$

The average particle size of CuO nanoparticles was found to be 17.3 nm calculated from β- full width at half maximum (FWHM) intensity of 0.5021 from the peak at θ-35.6^0. Further, the crystallite size of NiO nanoparticles was found to be between 3-4 nm using the

values of β- full width at half maximum (FWHM) intensity, 2.783 from the peak located at θ-43.3^0.

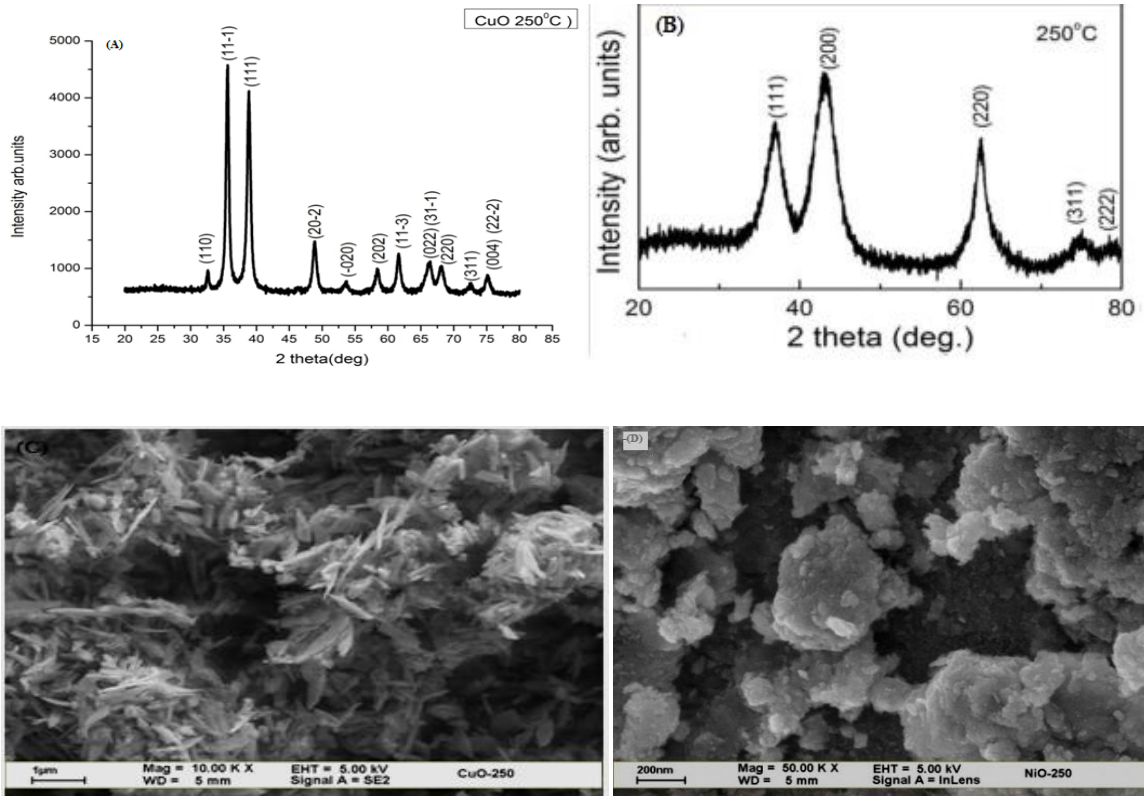

Figure 1. XRD of , A) CuO nano particles&B) NiO nano particlesand SEM images of, C) CuO nano particles & D) NiO nano particles

3.1.2. SEM morphological characterisation.

Fig 1(C) shows the SEM image of CuO nanoparticles and the surface morphology of the particles show irregular size, agglomerated nanoparticles appearing in sheet or rod like shapes. Such morphology imparts high surface area to the nanomaterial which intern will have high catalytic activity. The average particle size of CuOfrom SEM image is found to be 200 to 500 nm length and 20-30 nm width. Fig. 1(D) shows the SEM image of NiO nanoparticles having a spherical shape with an average particle size around 19 nm. The formation of ultrafine NiO nanoparticles reveals that high agglomeration of nanoparticles induces good catalytic activity.

3.1.3. IR and Raman studies.

Fig.2 (A) shows the FTIR spectrum of CuO nanoparticles which exhibit characteristic IR peaks at 523 cm^{-1}and 1011cm^{-1} indicating different modes of bending vibrations of the Cu–O bond. The peak at 1639 cm^{-1} is assigned to stretching vibration of the Cu–O bond of copper (II) oxide nanoparticles. The additional IR peaks at 2933 cm^{-1}and 3432 cm^{-1} belongs to the symmetric and asymmetric stretching vibration of the O–H bond respectively suggesting the presence of traces of water molecules. The FTIR spectrum of NiO nanoparticles is as shown in Fig. 2(B). The prominent peaks at 590 cm^{-1} and 610 cm^{-1} belongs to vibrations of Ni-O bond and other additional peaks at 1651 cm^{-1} and 3635 cm^{-1} are attributed to H-O-H stretching indicating trace amounts of moisture in the sample. The Raman spectrum of CuO nanoparticles

in Fig. 2(C) shows a characteristic peak around 981 cm^{-1} belonging to stretching mode of CuO while NiO nanoparticles in Fig. 2(D) exhibits a distinct peak at around 500 cm^{-1} related to stretching mode of NiO.

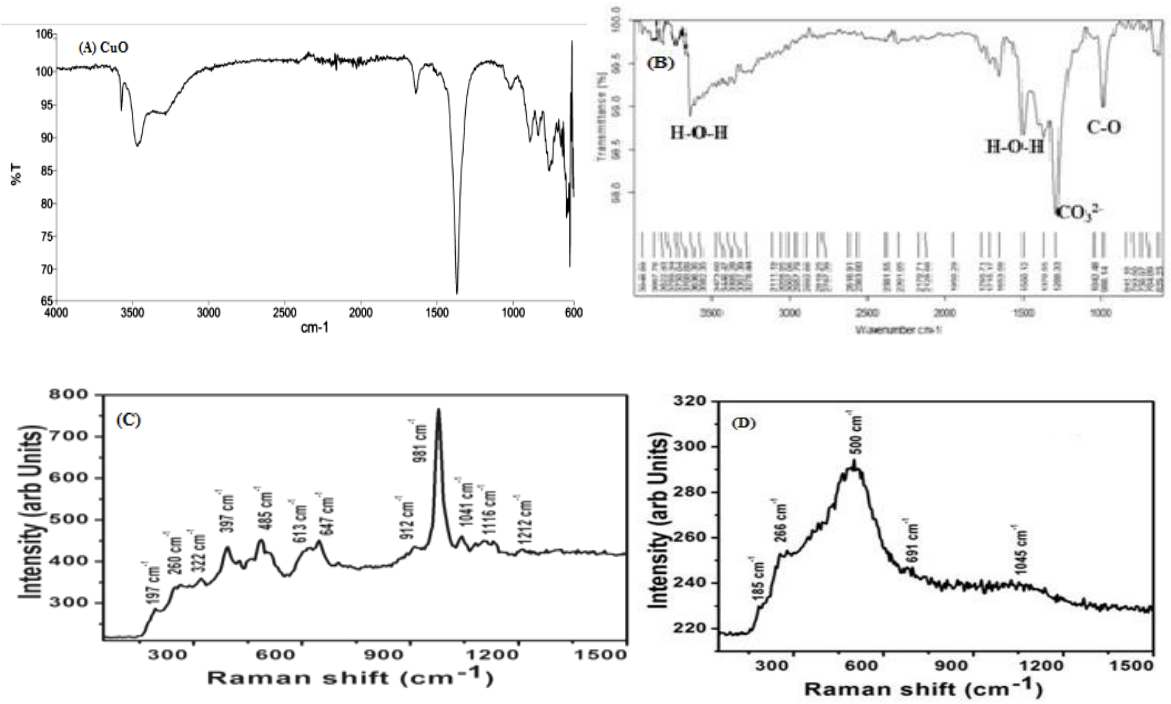

Figure 2. FTIR spectra of, A) CuO nanoparticles & B) NiO nanoparticlesand Raman spectra of C) CuO nanoparticles & D) NiO nanoparticles

3.2. Electrochemical behavior of DA and Tyr at CuO modified graphite electrode(CMG).

The metal oxide modified electrode was used to study the electrochemical oxidation of DA and Tyr using cyclic voltammetry. The experiments were performed in the presence of 500µM DA and 500µM Tyr individually at the modified electrode in PBS solution, pH 7.0 and results are compared with that on bare graphite electrode.

3.2.1. Electrochemical studies of DA at the CuO modified graphite electrode.

Fig. 3 (A) shows the cyclic voltammogram of 500µM DA at bare graphite electrode (a) and at CMG electrode (b) in PBS (pH=7.0) electrolyte. In PBS solution, pH 7.0 (in the absence of any analyte), the bare graphite electrode exhibits no obvious oxidation and reduction peaks (a) and the CuO modified electrode shows an anodic peak at -0.163 V and a cathodic peak at -0.355 V corresponding to oxidation (Cu^0/Cu^{+2}) and reduction (Cu^{+2}/Cu^0) of CuO nanoparticles respectively in PBS pH 7.0 solution. On the other hand, in the presence of 500 µM DA, DA undergoes reversible oxidation and reduction at bare graphite electrode with the oxidation peak located at about +0.257 V (c) and at the modified electrode, its oxidation peak is observed at +0.249 V. In addition, there is significant enhanced of oxidation peak current on the modified electrode indicating better electro catalytic behavior of CuO nanoparticles towards DA oxidation. The oxidation peak at +0.249 V on the CV curve of DA at the modified electrode is assigned to the formation of dopaminoquinone (DA^+) (product of dopamine oxidation) and the cathodic peak at +0.125 V is assigned to the reduction of DA^+ to leucodopanoquinone [42-43]. Fig 3(B) shows the CV profiles of DA at different concentrations and it is clear from the figure that the oxidation current of DA increases linearly with an increase in concentration at the CuO modified electrode.

3.2.1.1. Effect of scan rate.

In order to understand the reversibility of electrocatalytic oxidation reaction of DA at CuO modified electrode, cyclic voltametric experiments were conducted by varying scan rate from 20 to 200 mV s^{-1} as shown in Fig 3(C). A plot of I_{pa} vs. V shows a good linear relationship with zero intercept (inset in the figure) and another plot of anodic peak current (I_{pa}) varies linearly with square root of scan rate ($\upsilon^{1/2}$) (inset in the figure) with zero intercept. From both the plots, it is confirmed that the oxidation of DA at the CMG electrode is a diffusion controlled process. In order to calculate the kinetic parameters, a plot of E_{pa} vs. logV (Figure not shown) gives an anodic charge transfer coefficient (α) of 0.73 with slope equal to 2.303RT/(1-α)n_aF. The calculated Tafel slope, b for the modified electrode is found to be 0.034 V dec^{-1} whichwas less than theoretical value 0.118 V dec^{-1} for a one electron transfer process suggesting no adsorption of dopamine occurs on the electrode surface. From Laviron's equation (1) [44-45], electron transfer rate constant (k_s) for this CMG electrode was found to be 0.43 s^{-1} at 0.05 V s^{-1}.

$$\log k_s = \alpha \log (1-\alpha) + (1-\alpha) \log \alpha - \log (RT/nF n) - \alpha(1-\alpha)\, nFE/2.3RT \qquad (1)$$

According to the electron transfer kinetics, for any electron transfer process, higher the rate constant than 0.01 s^{-1}, then the reaction is fast and reversible. Hence the oxidation of DA at CMG electrode is fast, reversible and diffusion controlled with two proton coupled, two electron processes as shown in Fig 4.

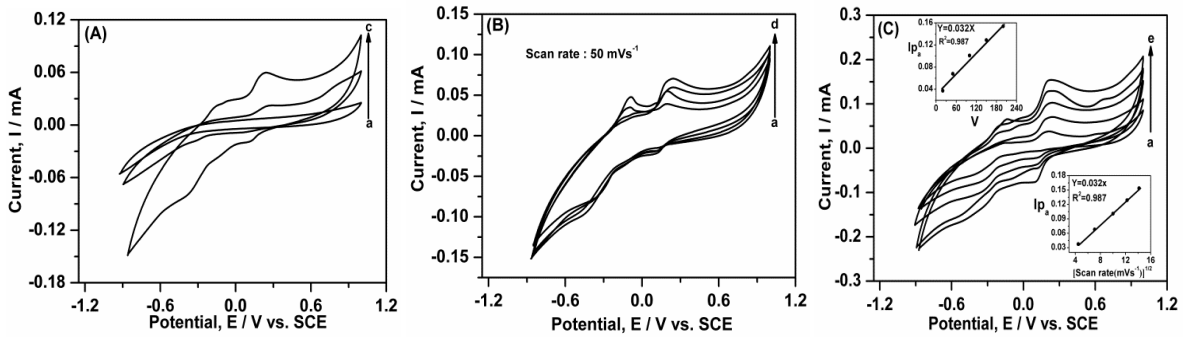

Figure 3. A) Cyclic voltammograms of: A) Bare graphite B) Bare graphite with 250 µM DA and 500 µM Tyr C) CMG WITH 250 µM DA: Electrolyte solution 0.1M Phosphate buffer solution (pH 7.0) + 0.1M KCl B) Cyclic voltammograms of DA of various concentrations at CMG electrode: a) 62.5 µM b)125 µM c)250 µM d)500 µM Scan rate: 50 mV s^{-1}C) Cyclic voltammograms of 500 µM DA at CMG electrode at different scan rates a) 20 b) 50 c)100 c)150 d)200 mV s^{-1} Inset: plots of I_{pa} vs υ and I_{pa} vs. $\upsilon^{1/2}$.

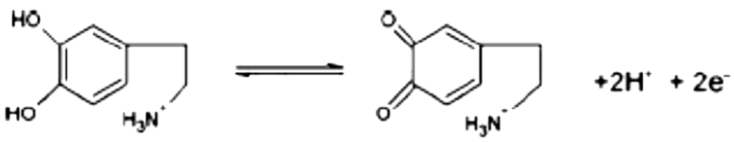

Figure 4. Oxidation of Dopamine (two electron process)

3.3. Electrochemical studies of L-Tyrosine at CuO modified electrode.

Fig.5(A) shows the electrochemical behavior of Tyr at the CMG modified electrode. Tyr undergoes irreversible oxidation at the modified electrode with an anodic peak at 0.812 V with an enhanced peak current compared to that at the bare graphite electrode. The enhancement in the anodic peak current suggests that the CuO modified electrode shows good

electro catalytic activity towards Try oxidation. Fig 5(B) shows the CV profile of Tyr at the CuO modified electrode and it observed that the oxidation current of DA increases linearly with increase in concentration. To understand the effect of scan rate, cyclic voltammetry profiles were recorded at CMG in PBS 7.0 solution containing 250 µM tyrosine and are as shown in Fig.5(C). Using *Randels- Sevcik* equation, a plot of I_{pa}vs. $\upsilon^{1/2}$ (20 to 200 mV s^{-1}) shows good a linear relationship with zero intercept, $I_{pa} = 0.0205\ \upsilon^{1/2}$ (Inset in the figure). Thus electrochemical oxidation of Tyr at CMG electrode is diffusion controlled process and exhibits irreversibility which was also confirmed from shifting of anodic peak potential towards a more positive potential.

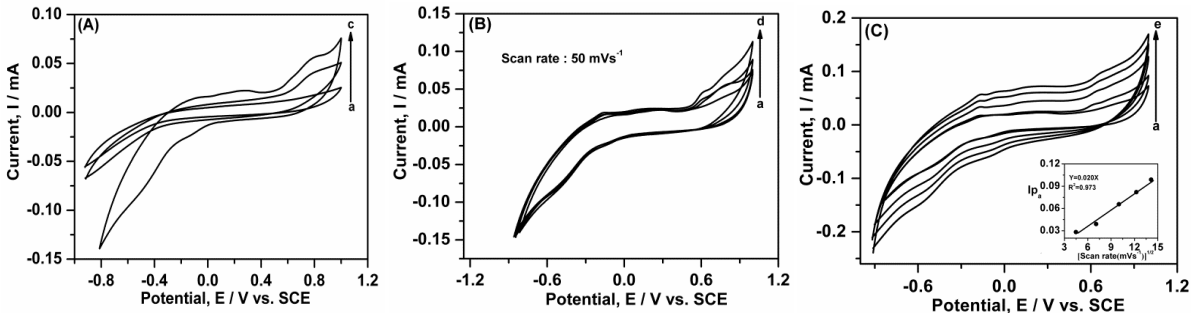

Figure 5. A) Cyclic voltammograms of: A) Bare graphite B) Bare graphite with 500 µM Tyr C) CMG with 500 µM Tyr: Electrolyte solution 0.1M Phosphate buffer solution (pH 7.0) + 0.1M KCl B) Cyclic voltammograms of Tyr of various concentrations at CMG electrode: a) 250 µM b)500 µM c)750 µM d)1000 µM Scan rate: 50 mV s^{-1}C) Cyclic voltammograms of 250 µM Tyr at CMG electrode at different scan rates a) 20 b) 50 c)100 c)150 d)200 mV s^{-1} Inset: plot of I_{pa} vs. $\upsilon^{1/2}$.

3.4. Simultaneous determination of DA, AA and Tyr using CuO modified graphite electrode.

Since DA and AA coexist in the biological fluids, interference of one in the determination of others and also in the presence of a very low concentration of tyrosine during their selective determination cannot be ruled out. It is understood that high concentrations of DA and AA may interfere with the detection of Tyr. Further, the poor response of tyrosine and combined response of DA and AA at very close potentials are generally observed on bare electrodes. The CV studies were conducted for ternary mixture of 500 µM DA, 2 mM AA and 500 µM Tyr in PBS buffer solution at bare graphite electrode and CuO modified graphite electrode and results are as shown in Fig. 6. On bare graphite, there was convergence of oxidation peaks of AA, DA and Tyr was noticed which cannot provide any information about concentration of individual analytes. Conversely, oxidation peaks of AA, DA and Tyr are very well separated from one another and appear at different potentials, 193 mV, 359 mV and 682 mV respectively. In addition, an additional peak was observed at -131 mV which corresponds to Cu^0/Cu^{+2} redox couple of copper oxide nanoparticles. CV studies from Fig. 6(A) shows that all the analytes in the ternary mixture are clearly distinguishable and the anodic peak potential differences between AA-DA, DA-Tyr and AA- Tyr were 166 mV, 323 mV and 489 mV respectively. On the other hand, DPV studies of the same ternary mixture of 500 µM DA, 2 mM AA and 500 µM Tyr in PBS buffer solution at bare graphite electrode are as shown in Fig. 6(B). From the figure, it is clear that anodic peaks corresponding to AA, DA and Tyr is submerged and appears as broad single peak with a low anodic current at bare graphite (a). On contrary, on CuO modified graphite electrode(c), the anodic peaks corresponding to AA, DA and Tyr are clearly separated and three distinguishable anodic peaks are observed. The peak potential separations between, AA-DA, DA-Tyr and AA-Tyr in DPV are found to be 209 mV,

400 mV and 609 mV respectively. From the above discussion, it is clearly proved that the CuO modified graphite electrode was able to separate the anodic oxidation current signals of DA, AA and Try and exhibits good electro-catalytic activity compared to that of the bare graphite electrode.

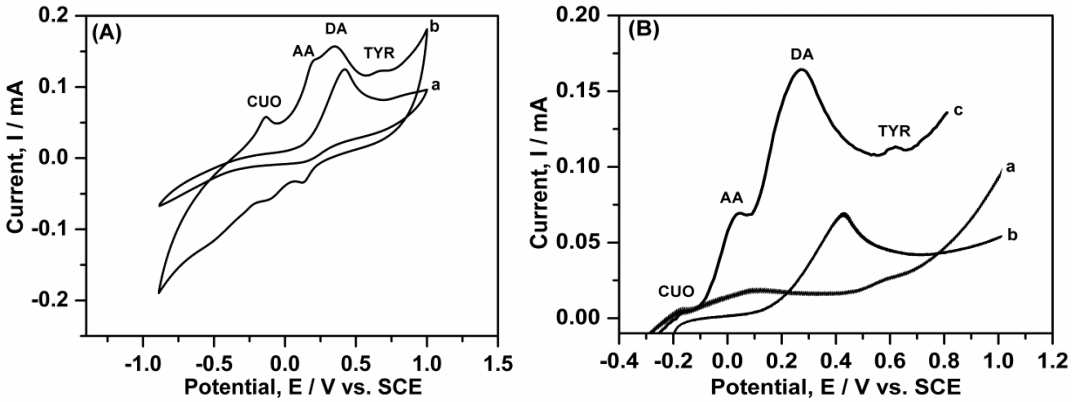

Figure 6. A) Cyclic voltammograms of a) Bare graphite with DA 500 µM, 500 µM Tyr and 2 mM AA b) CMG graphite with 500 µM DA, 500 µM Tyr and 2 mM AA; Scan rate 50 mV s^{-1} B) Differential pulse voltammogram of a) Bare graphite with 500 µM DA, 500 µM Tyr and 2 mM AA b) CMG electrode with no analyte c) CMG graphite with 500 µM DA, 500 µM Tyr and 2mM AA

3.4. Electrochemical behavior of Tyr at NiO modified graphite electrode (NMG).

Due to the high electrocatalytic activity of NiO nanoparticles, electrochemical studies were conducted for the detection of tyrosine using NiO modified graphite electrode in PBS solution, pH 7.0. The CV profiles were recorded at NiO modified graphite electrode at different concentrations of Tyr in the range of 5 to 400 µM in PBS pH 7.0 and are as shown in Fig 7(A). From the figure, it can be seen that the oxidation peak of Tyr appears at +0.80 V and the peak current increases with an increase of concentration of tyrosine confirming an excellent electrocatalytic activity of NiO modified electrode towards oxidation of DA. In order, to understand electron transfer kinetics of oxidation reaction of Tyr at NMG, CV studies were performed with varying scan rate in the range 20 to 200 mVs^{-1} and the results are shown in Fig. 7(B). A plot I_{pa} vs. square root of scan rate, (from *Randels-Sevcik* equation) shows a good linear relationship with zero intercept, (inset in the figure) indicating the reaction goes through diffusion controlled process rather than charge controlled process.

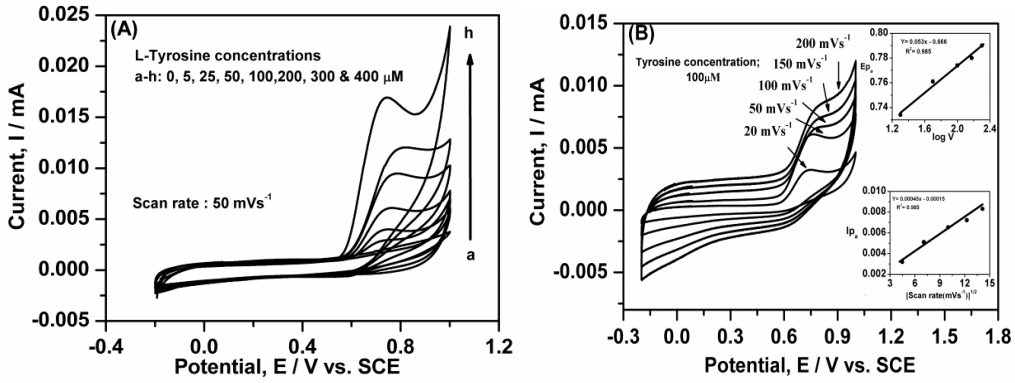

Figure.7. A) Cyclic voltammograms of Tyr of various concentrations at NMG electrode a) 0 b) 5 c) 25 d) 50 e) 100 f) 200 g)300 h) 400 µM 50 mV s^{-1} B) Cyclic voltammograms of 100 µM Tyr at NMG electrode at different scan rates a)20 b)50 c)100 d)150 e) 200 mVs^{-1} Inset: plots of I_{pa} vs υ and I_{pa} vs. $\upsilon^{1/2}$.

From Fig 7(B) it is found that anodic peak of Try shifts towards the positive side of potential suggesting irreversibility of electrochemical reaction. The slope of E_{pa} vs. logV is equal to 2.303RT/(1-α)n_aF (from inset in the Fig 7(B)) is used to calculate the charge transfer coefficient, α and was found to be 0.140 for NiO modified electrode. The calculated Tafel slope, b, for the irreversible diffusion controlled process was 0.112 $Vdec^{-1}$ and it is close to the theoretical Tafel value of 0.118 $Vdec^{-1}$ for one electron reaction. Thus the electrochemical oxidation of tyrosine at NMG is a one electron transfer process in accordance with the equation in Fig. 8.

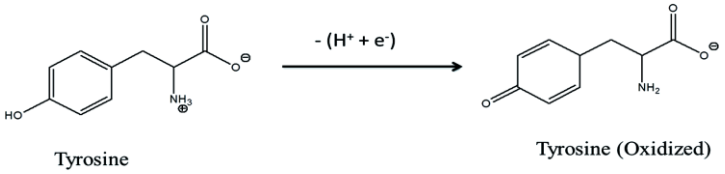

Figure 8. Oxidation of tyrosine (one electron transfer)

3.5. A comparative electrochemical study of MO (M=Cu and Ni) modified graphite electrode on dopamine and tyrosine.

A comparative account of the electrochemical performance of NiO and CuO modified graphite electrodes towards the electrochemical oxidation of 500 µg dopamine and Tyrosine - 250 µg are as shown in Fig. 9(A) and Fig 9(B) respectively. The evaluated electrochemical parameters from the study are provided in table 1.Taking into consideration of aforementioned electrochemical parameters in table 1 for CuO and NiO modified graphite electrodes towards oxidation of dopamine and tyrosine, CMG shows high catalytic activity and sensing performance than NMG. Despite having a high surface area to volume ratio, NiO exhibits sheet and charge transfer resistance which decreases the electrical conductivity which leads to poor catalytic or sensing activity [46]. On the other side, due to the high redox potential and low over potential, CuO oxidize dopamine and tyrosine with high anodic potential and at lower potentials compared to NiO.

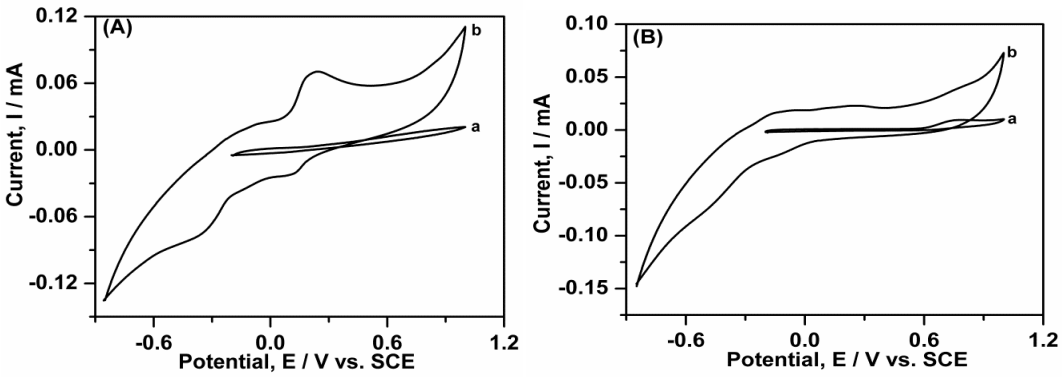

Figure 9. A) Cyclic voltammogram of 500 µM DA at a) NMG electrode b) CMG electrode B) Cyclic voltammogram of 250 µM Tyr at a) NMG electrode b) CMG electrode 50 mV s^{-1}.

3.6. Stability and Reproducibility.

The stability and reproducibility of NiO and CuO modified graphite electrodes were evaluated in separate experiments by measuring their cyclic voltammetry response upon storing for 1-4 weeks.. The modified electrodes were used for the selective detection of 500 µM DA in presence of 500 µM Tyr and 2 mM AA in PBS pH 7.0. The CuO modified graphite electrode could distinguish the (Figures not shown) oxidation peaks of DA, AA and Tyr in their ternary

mixture and shows good response to the selective determination of DA retaining 93, 90, 86 and 82% of its initial current response when stored for 1,2,3 and 4 weeks respectively. To ensure the reproducibility of the results, experiments were performed with the same CuO modified electrode for repeated measurement of 100 µM DA using chronoamperommetry. After each measurement the modified electrode was washed in PBS pH 7.0 and transferred into another standard solution of 100 µM DA to record its oxidation peak current. It is found that the modified electrode lost 8.9 % of initial amperometric response after 15 repeated measurements at a constant dopamine concentration of 100 µM and the step potential applied was 500 mV. Another experiment was conducted with a single modified electrode and the standard deviation for 10 successive scans was less than 5% in PBS pH 7.0 solution containing 20 mM DA. This indicates the excellent reproducibility of the CuO modified electrode. On the other hand, under similar experimental conditions, NiO modified graphite electrode retained 92, 89, 85 and 80% of its initial current response when stored for 1,2,3 and 4 weeks respectively for the oxidation of 100 µM DA. NiO modified electrode lost 10.1 % of initial amperometric response after 15 repeated measurements at a constant dopamine concentration of 100 µM and standard deviation for successive scan at a constant concentration of 20 mM DA was less than 7%.

Table 1. Electrochemical parameters on MO (M=Cu and Ni) modified graphite electrode on detection of DA and Tyr.

Analyte / Electrode	Dopamine-500 µM		Tyrosine -250 µM	
	I_{Pa} (mA)	E_{pa} (V)	I_{Pa} (mA)	E_{pa} (V)
CMG	+0.07019	+0.229	+0.0416	+0.80
NMG	No specific anodic peaks were identified		+0.0094	+0.80

4. Conclusions

Copper oxide nanoparticles prepared by sol-gel method were sucecesfully used for the fabrication of CuO modified graphite electrode which exhibitedgood electrocatalytic activity towards oxidation of AA, DA and Tyr. Cyclic voltammetry and differential pulse voltammetry studies revealed that oxidation peaks of DA, AA and Tyr are very well separated with high current sensitivity and good stability, particularly for DA. On the other hand, NiO modified electrode displays poor activity towards dopamine but shows good sensitivity towards the determination of tyrosine. Among, the two metal oxides used for the determination of DA, the CuO modified electrode shows high catalytic activity. For Tyr, NiO modified graphite electrode is found to be having good electrocatalytic activity. No electrode fouling was observed upon electro-oxidation of DA in the presence of Tyr or high concentration of AA at the CuO modified graphite electrode.Finally, CuO modified electrode demonstrated remarkarable sensing activity towards multianalyte mixture of DA, AA and Tyr.

Funding

This research was funded by Science and Engineering Research Board-Department of Science and Technology (SERB-DST), grant number ECR/2016/000644.

Acknowledgments

Authors are grateful to the Management of GITAM (Deemed to be University), Bangaluru Campus, India.

Conflicts of Interest

The authors declare no conflict of interest.

References

1. Choudhury,A.; Tripti, S.; Praveena, L.R.; Banerjee, A.K.; Indrajeet, C.; Arun Kumar, R.; Neelima, A. Neurochemicals, behaviours and psychiatric perspectives of neurological diseases. *Neuropsychiatry* **2018** , *8*, 395-424, https://doi.org/10.4172/Neuropsychiatry.1000361.
2. Bo, S.; Edward, S. Recent Advances in the Detection of Neurotransmitters. *Chemosensors* **2018**, *6*, 1-24, https://doi.org/10.3390/chemosensors6010001.
3. Dalley, J.W.; Roiser, J.P. Dopamine, serotonin and impulsivity. *Neuroscience* **2012**, *215*, 42-58, https://doi.org/10.1016/j.neuroscience.2012.03.065.
4. Marianne O.K.; Daniella, S.B.; Ariel, R.C.; David, N.H.; Jackson, C.B.; Ricardo, G.C. Dopamine: Functions, Signaling, and Association with Neurological Diseases. *Cellular and Molecular Neurobiology* **2019,** *39*, 31-59,https://doi.org/10.1007/s10571-018-0632-3.
5. Kesby, J.P.; Eyles,D.W.; McGrath,J.J.;Scott, J.G. Dopamine, psychosis and schizophrenia: the widening gap between basic and clinical neuroscience. *Transl. Psychiatry***2018**, *8*,https://doi.org/10.1038/s41398-017-0071-9.
6. Kang, Y.J.;Cutler, E.G.; Cho, H. Therapeutic nanoplatforms and delivery strategies for neurological disorders. *Nano Converg* **2018,** *5*,https://doi.org/10.1186/s40580-018-0168-8.
7. Kapalka, G. Substances Involved in Neurotransmission. In:*Nutritional and Herbal Therapies for Children and Adolescents.*1st Ed., Academic Press is an imprint of Elsevier, London, UK,Chapter 4, **2010**; pp. 74-99,https://doi.org/10.1016/C2009-0-01890-X.
8. Heiko, B.; Sabine,J.K.; Birgit, A.; Thomas, O. Inherited Disorders of Neurotransmitters: Classification and Practical Approaches for Diagnosis and Treatment. *Neuropediatrics* **2019,** *50*, 2-14, https://doi.org/10.1055/s-0038-1673630.
9. Ferguson, A.A.; Roy,S.; Kaitlyn, N. K.; Yongsoon, K.; Dumas, K.J.; Ritov, V.B.; Matern, D.; Patrick J.H.; Fisher, A.L.TATN-1 Mutations Reveal a Novel Role for Tyrosine as a Metabolic Signal That Influences Developmental Decisions and Longevity in *caenorhabditis elegans. PLOS Genetics* **2013**, *9*, 1-22, https://doi.org/10.1371/journal.pgen.1004020.
10. Mohorko, N.; Petelin, A.; Jurdana, M.; Gianni, B.; PraDnikar, Z.J. Elevated Serum Levels of Cysteine and Tyrosine: Early Biomarkers in Asymptomatic Adults at Increased Risk of Developing Metabolic Syndrome.*BioMed Research International* **2015**,*2015*,1-14, http://dx.doi.org/10.1155/2015/418681.
11. Zahra, T.A.; Oana, H.; Cecilia, C.; Mohammad, M.A.; Giovanna, M. Latest Trends in Electrochemical Sensors for Neurotransmitters: A Review. *Sensors* **2019**, *19*, 1-30, https://doi.org/10.3390/s19092037.
12. Govindhan, M.; Manickam, S.; Vellaichamy, G. Electrochemical sensor and biosensor platforms based on advanced nanomaterials for biological and biomedical applications. *Biosensors and Bioelectronics* **2018**, *103*, 113–129, https://doi.org/10.1016/j.bios.2017.12.031.
13. José, A.R.; Paula, M.V.F.; Carlos, M P.; Silva, F. Electrochemical Sensors and Biosensors for Determination of Catecholamine Neurotransmitters: a Review. *Talanta* **2016**, *160*,1-87, http://dx.doi.org/10.1016/j.talanta.2016.06.066.
14. Sara, A.A.; Mahmoud, A.H.; Aisha, A.G.; Anish, K. Composite Material–Based Conducting Polymers for Electrochemical Sensor Applications: a Mini Review. *BioNanoSci.* **2020**, *10***,** 351–364, https://doi.org/10.1007/s12668-019-00708-x.
15. Cheng, Y.; Madelaine, E.D.; Poojan, P.B.; Jill, V. Recent trends in carbon nanomaterial-based electrochemical sensors for biomolecules: A review. *Analytica Chimica Acta* **2015**, *887*, 17-37, https://doi.org/10.1016/j.aca.2015.05.049.
16. Wan, Q.L.; Zhiqiang, G. Metal oxide nannoparticles in electroanalysis. *Electroanalysis* **2015**, *27*, 1-18, https://doi.org/10.1002/elan.201500024.
17. Manjunatha, H.; Nagaraju, D.H.; Suresh, G.S.; Venkatesha, T.V. Detection of Uric Acid in the Presence of Dopamine and High Concentration of Ascorbic Acid Using PDDA Modified Graphite Electrode. *Electroanalysis* **2009**, *21*, 2198–2206, https://doi.org/10.1002/elan.200904662.
18. Muhammad, S.; Mazen, K.N; Muhammad, M.; Abdulnaser, A.; Shehzada, M.S.J.; Chanbasha, B. Chemically modified electrodes for electrochemical detection of dopamine in presence of uric acid and ascorbic acid: A review. *Trends in Analytical Chemistry* **2015**, *76*, 15-26, https://doi.org/10.1016/j.trac.2015.09.006.
19. Intan, R.S.; Novi, A.; Tae, Kim, H. Nanomaterial-modified Hybrid Platforms for Precise Electrochemical Detection of Dopamine.*BioChip J*. **2019**, *13*, 20-29, https://doi.org/10.1007/s13206-019-3106-x.
20. Yingchun, L.; Rongyan, H.; Yan, N.; Fei, L. Paper-Based Electrochemical Biosensors for Point-of-Care Testing of Neurotransmitters. *Journal of Analysis and Testing* **2019,** *3*, 19-36, https://doi.org/10.1007/s41664-019-00085-0.

21. Krystyna, J.; Pawel, K. New trends in the electrochemical sensing of dopamine. *Anal Bioanal Chem.* **2013,***405*, 3753–3771, https://doi.org/10.1007/s00216-012-6578-2.
22. Mathieu, O.; Jessy, M.; Niyonambaza, S.D.; Miled, A.; Elodie, B. Electrochemical Detection of Dopamine Based on Functionalized Electrodes. *Coatings* **2019**, *9*, 496, https://doi.org/10.3390/coatings9080496.
23. Hadi, B.; Mohadeseh, S.; Somayeh, T.Different Electrochemical Sensors for Determination of Dopamine as Neurotransmitter in Mixed and Clinical Samples: A Review. *Anal. Bioanal. Chem. Res* **2019**, *6*, 81-96, https://doi.org/10.22036/ABCR.2018.142219.1229.
24. Zhang, H.; Zhu, Q.; Zhang, Y. One-pot synthesis and hierarchical assembly of hollow Cu_2O microspheres with nanocrystals-composed porous multishell and their gas-sensingproperties. *Adv Funct Mater* **2007**, *17*, 2766–2771, https://doi.org/10.1002/adfm.200601146.
25. Tarascon, J.M.; Poizot, P.; Laruelle, S. Nano-sized transition-metal oxides as negative-electrode materials for lithium-ion batteries. *Nature* **2000**, *407*, 496–499, https://doi.org/10.1038/35035045.
26. Zhang, J.; Liu, J.; Peng, Q. Nearly monodisperse Cu_2O and CuO nanospheres: preparation and applications for sensitive gas sensors. *Chem Mater* **2006,***18*, 867–871, https://doi.org/10.1021/cm052256f.
27. Bayoumy, A.M; Elhaes, H; Osman, O; Kholmurodov, K.T; Hussein. T; Ibrahim, M.A. Effect of nano metal oxides on heme molecule: molecular and biomolecular approaches. *Biointerface Res. Appl. Chem.* **2020**, *10*, 4837 – 4845, https://doi.org/10.33263/BRIAC101.837845.
28. Zhang, X.; Wang, G.; Liu, X. Different CuO nanostructures: synthesis, characterization, and applications for glucose sensors. *J Phys Chem C* **2008**, *112*, 16845–16849, https://doi.org/10.1021/jp806985k.
29. Shafiee, M.R.M; Kargar, M. Preparation of aryl sulfonamides using CuO nanoparticles prepared in extractive rosmarinus officinalis leaves media, *Biointerface Res. Appl. Chem.* **2016**, *6*, 1257-1262.
30. Yazid, S.N.A.M.; Illyas, M. I.; Suriani, A. B.; Norhayati, H.;Sazeli, A G.A Review of Glucose Biosensors Based on Graphene/Metal Oxide Nanomaterials. *Analytical Letters* **2014**, *47*,1821-1834, https://doi.org/10.1080/00032719.2014.888731.
31. Taher, A.; Shabnam, M. A Nafion-free nonenzymatic amperometric glucosesensor based on copper oxide nanoparticles-graphene nanocomposite. *Sensors and Actuators B: Chemical* **2014**,*198*, 438-447, https://doi.org/10.1016/j.snb.2014.03.049.
32. Yunxia, Z.; Xiaodan, Z.; Qiumeng, C. S. Li.; Haiyan, C.; Yuming, H. Co_3O_4/CuO hollow nanocage hybrids with high oxidase-like activity for biosensing of dopamine. *Materials Science & Engineering C* **2019**, *94*, 858–866, https://doi.org/10.1016/j.msec.2018.10.038.
33. Huang, Y.; Tan, Y.; Feng, C.; Wang, S.; Wu,H.; Zhang, G. Synthesis of CuO/g-C_3N_4 composites, and their application to voltammetric sensing of glucose and dopamine. *Microchim Acta* **2019**,*186,* https://doi.org/10.1007/s00604-018-3120-z.
34. Felixa, S.; Santhosh, C.; Nirmala, G.A.CuO-MWCNTS for Enzyme-Less Electrochemical Detection of Glucose and Dopamine.*ECS Transactions* **2017**, *77*, 1847-1857, https://doi.org/10.1149/07711.1847ecst.
35. Baloach, Q.; Ayman, N.; Aneela, T.; Sirajuddin; Syed, T.H.S.; Tayyaba, S.; Munazza, A.; Willander, M.; Zafar, H.I. An amperometric sensitive dopamine biosensor based on novel copper oxide nanostructures, *Microsystem Technologies* **2017**, *23*,1229–1235, https://doi.org/10.1007/s00542-015-2805-z.
36. Hulya, O.D.; Bingul, K.U.; Emir, C.; Mesut, E. Simultaneous electrochemical detection of ascorbic acid and dopamine on Cu_2O/CuO/electrochemically reduced graphene oxide (Cu_xO/ERGO) nanocomposite-modified electrode. *Microchemical Journal* **2019**,*150*, https://doi.org/10.1016/j.microc.2019.104157.
37. Wenxiu, G.; Miaomiao,W.X.M.; Yuru, W.; Lei, L.; Wenshui, X. A facile sensitive L-tyrosine electrochemical sensor based on a coupled CuO/Cu_2O nanoparticles and multi-walled carbon nanotubes nanocomposite film. *Anal. Methods* **2015,** *7*, 1313-1320, https://doi.org/10.1039/C4AY01925C.
38. Asghar, P.; Akbarzadeh-Torbati, N.; Beitollahi, H. Rapid and Sensitive Electrochemical Monitoring of Tyrosine Using NiO Nanoparticles Modified Graphite Screen Printed Electrode. *Int. J. Electrochem. Sci.* **2019**, *14*, 1556 – 1565, https://doi.org/10.20964/2019.02.42.
39. Faezeh, S-F; Roushani, M. Architecting of a biodevice based on a screen-printed carbon electrode modified with the NiO NP nanolayer and aptamer in BCM-7 detection. Colloids and Surfaces B: Biointerfaces **2020**, *190*,110932, https://doi.org/10.1016/j.colsurfb.2020.110932.
40. Hong, Y.Y.; Zhang, H.J.; Huang, S.; Gao, X.; Shan, S.S.; Wang, Z.; Wang, W.Q.; GuaN, E.H. A novel non-enzymatic dopamine sensors based on NiO-reduced graphene oxide hybrid nanosheets. *Journal of Materials Science: Materials in Electronics*. **2019**, 30, 5000–5007,https://doi.org/10.1007/s10854-019-00796-1.
41. Anuprathap, M.U.; Srivastava, R. Synthesis of $NiCo_2O_4$ and its application in the electrocatalytic oxidation of methanol. *NanoEnergy* **2013**,*2*,1046-1053,https://doi.org/10.1016/j.nanoen.2013.04.003.
42. Valenzuela, M.V.; Huerta, F.; Morallón, E.; Montilla,F. Affinity of Electrochemically Deposited Sol–Gel Silica Films towards Catecholamine Neurotransmitters. *Sensors* **2019**, *19*, 868,1-15,https://doi.org/10.3390/s19040868.
43. Fayemi, O.E.; Adekunle, A.S.; Kumara Swamy, B.E.; Ebenso, E.E. Electrochemical sensor for the detection of dopamine in real samples using polyaniline/NiO, ZnO, and Fe3O4 nanocomposites on glassy carbon electrode. *Journal of Electroanalytical Chemistry* **2018,** *818*, 236-249, https://doi.org/10.1016/j.jelechem.2018.02.027.

44. Bard, A.J.; Faulkner, L.R. *Electrochemical Methods, Fundamentals and Applications*. 2nd Ed. Wiley, New York.2006.
45. Laviron, E. General expression of the linear potential sweep voltammogram in the case of diffusionless electrochemical systems. *J. Electroanal. Chem. Interfacia Electrochem*. **1979**, *101*, 19–28, https://doi.org/10.1016/S0022-0728(79)80075-3.
46. George, J.M.; Arun, A.; Mathew, B. Metal oxide nanoparticles in electrochemical sensing and biosensing: a review.*Microchim Acta* **2018**, *185*,https://doi.org/10.1007/s00604-018-2894-3.